Anti-Jamming Resilient LEO Satellite Swarms

Venkata Srirama Rohit Kantheti [†], Chia-Hung Lin [†], Shih-Chun Lin [†] and Liang C. Chu [‡]

[†]Intelligent Wireless Networking (iWN) Laboratory, Department of Electrical and Computer Engineering

North Carolina State University, Raleigh, NC 27695, USA

[‡]Lockheed Martin Space, Sunnyvale, CA 94089, USA

Email: vkanthe@ncsu.edu, clin25@ncsu.edu, slin23@ncsu.edu, liang.c.chu@lmco.com

Abstract-Advancements in wireless communication and electronics in the past decade have propelled the incorporation of non-terrestrial platforms into mainstream communication networks, opening avenues for several new frontier applications. Notably, low earth orbit (LEO) satellite deployments are being proposed for ubiquitous connectivity, both in commercial and military applications, owing to the possibility of rapid prototyping and deployment. This paper introduces an LEO satellite orchestration framework that provides a satellite swarm system with innovative multi-node coordination designs, namely d-MRC and d-LMMSE, to enhance communication capacity while preserving robustness against jamming adversaries. A hardware-in-the-loop testbed has been built with universal software radio peripheral radios and over-the-air transmissions, which closely emulate realworld satellite communications channels. Experimental results with real-time transmissions validate the effectiveness of our designs as compared to single LEO satellite operations.

Index Terms—Low earth orbit satellite communication, satellite swarms, eigen-spatial processing, receiver diversity, antijamming, and hardware-in-the-loop testbed.

I. INTRODUCTION

The advent of six-generation (6G) and beyond communications makes the vision of ubiquitous global connectivity a feasible reality. Towards this end, LEO satellites provide an attractive solution by enabling many deployments in the form of a swarm of nodes, which is possible due to rapid prototyping and manufacturing. Through swarm deployments, they also build resistance to network outages, enable low-latency communication compared to traditional higher-orbit satellite deployments, facilitate jamming resilience, and provide an infrastructure for cross-layer intelligent network frameworks in the satellite communication paradigm [1].

Adding onto the highly prevalent commercial use cases for LEO architectures [2]–[4], the Space Development Agency (SDA) is in the process of building a "proliferated warfighter space architecture" using numerous such satellites for tactical needs [5]. This architecture heavily relies on deploying proliferated LEO constellations in a small number of orbits, with a focus on enabling intelligent beyond-line-of-sight (BLOS) communication.

Despite their advantages, LEO deployments also come with certain communication challenges [6]–[8]. A prominent aspect is a highly prevalent line-of-sight (LOS) channel between

This work was supported in part by Lockheed Martin Space, the North Carolina Space Grant, the North Carolina Department of Transportation under Award TCE2020-03, the National Science Foundation under Grant CNS-221034, Meta 2022 AI4AI Research, and Cisco Research.

ground terminals and the satellite nodes, especially in the nonurban areas [9]. This implies a lack of diversity in the wireless channels for implementing single-input multi-output (SIMO) and multi-input multi-output (MIMO) communications. Such a predicament can, however, be mitigated when using distributed deployments to form swarm satellite systems.

Introducing diversity into communication also aids in building jamming resilience to a certain extent. Due to the nature of cyclic visibility and fixed orbits [10], satellites are prone to jamming attacks. Anti-jamming (AJ) is vital in any wireless communication paradigm and is a well-researched topic. Traditional spread spectrum techniques such as direct sequence and frequency-hopping spread spectrums have been widely used in the literature. One can exploit the diversity in a swarm setting in satellite communication to alleviate the jammers' influence [11], [12].

In line with this motivation, we aim to utilize the concept of LEO constellation deployments to build a distributed receiver system, where each satellite node in a swarm can act as part of a larger receiver. This introduces diversity into the communication, enabling SIMO/MIMO in ground-to-space uplink connections. On the flip side, such an architecture can also be explored further for building intelligent distributed networks that can support energy-efficient multi-node coordination [13] and statistical quality-of-service guarantees in a large cognitive system [14].

In this paper, we intend to exploit the diversity in the proposed receiver system to perform two operations. First is to improve the received effective SNR and data rates, and second is to build robustness in the entire system against external jamming. For this purpose, we utilize two schemes: a distributed maximal ratio combining (d-MRC) operation for improving the overall receiver data rates and a distributed linear minimum mean square error combining (d-LMMSE) method that provides anti-jamming capabilities.

To prove the effectiveness of these operations, a hardware system is first realized using the universal software radio peripheral (USRP) X310 radios in an indoor environment. We show that an indoor testbed can realize approximate LOS yet diverse channels. Then, we evaluate the d-MRC and d-LMMSE schemes on our software-defined radio (SDR) testbed. AJ capability is evaluated by generating different jamming signals using a signal generator near the testbed.

The rest of the paper is organized as follows. Section II details the system architecture and the utilized theoretical

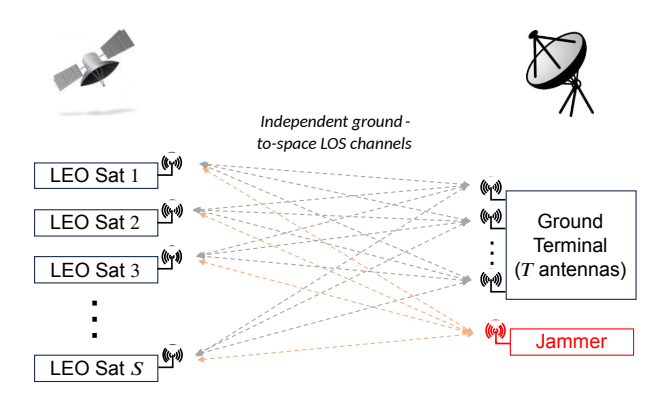


Fig. 1. The proposed LEO swarm system architecture.

channel model. Section III gives a mathematical background for the d-MRC and d-LMMSE schemes. Section IV provides our USRP testbed setup emulating satellite channels in an indoor environment. Section V presents the performance evaluation of our designed multi-node schemes on over-the-air (OTA) data, and Section VI concludes the paper.

II. DISTRIBUTED SWARM SATELLITES IN SPACE

This section introduces our proposed system architecture shown in Fig. 1 where S LEO satellites are deployed in a known orbit, and a single unit acts as a ground terminal G. Each LEO satellite is assumed to host a single antenna, and all the S satellites collectively represent one S-antenna distributed receiver. The ground terminal can use one or more antennas, represented by the count T. This paper will limit T=1 to demonstrate SISO/SIMO operations and AJ resilience. A malice jammer on the ground is shown to interfere with the satellites. Since the satellite orbits are fixed, a jammer can use this to jam several satellites in the same or different orbits by intelligently managing operating time.

A. Beyond-Line-of-Sight Satellite Channel Model

Let us begin by considering a pure LOS ground-to-space SISO communication scenario. Owing to the nature of wireless communications, the transmitted data gets distorted due to frequency and timing offsets, channel phase offsets, additive noise, and external interference (such as jammers) before reaching the receivers. We assume that our SISO link is operating in the presence of an external jammer. The captured baseband data at i^{th} satellite node, after downsampling and eliminating frequency and timing offsets, can be represented as $\mathbf{r}_i[k] \in \mathbb{C}^{1 \times \tau}$ [15]–[17]:

$$\mathbf{r}_{i}[k] = \sqrt{p_{q}}h_{i}\mathbf{x}[k] + \sqrt{p_{j}}h_{j,i}\mathbf{x}_{j}[k] + \mathbf{n}_{i}$$
 (1)

where p_g and p_j represent the ground terminal transmit power and jammer transmit power, respectively; h_i represents the SISO channel and $h_{j,i}$ is the channel distortion caused by the jammer on i^{th} LEO receiver respectively; $\mathbf{x}[k]$ and $\mathbf{x}_j[k]$ represent the transmitted frame from the ground terminal and the jammer, both with a size of τ samples (i.e. $\mathbb{C}^{1 \times \tau}$); and \mathbf{n}_i is the independent and identically distributed (i.i.d.) noise component.

Since the LEO communication is void of strong multipath components, the channel can be modeled in terms of the total path loss, which depends on the free space path loss, attenuation due to atmospheric gases, tropospheric/ionospheric scintillation, shadow fading, and clutter loss [9], [18].

Then the SISO channel is obtained as [7]:

$$h = \frac{1}{\sqrt{PL}} e^{-j(\theta_{\text{atm,i}} + \nu d)}, \tag{2}$$

where PL is the path loss, $\nu = 2\pi f_c/c_0$ is the wave number of the transmitted signal, f_c is the center frequency, c_0 is the speed of light, and $\theta_{\rm atm,i}$ is the uniform distributed phase offset due to atmosphere at satellite i.

Now, for a SIMO mode of operation consisting of T=1 transmit antennas at the ground terminal and S single-antenna LEO nodes, the wireless channel is represented as a vector

$$\mathbf{h} = [h_1, h_2, \dots h_S]^T \in \mathbb{C}^{S \times 1}.$$

III. ANTI-JAMMING-ENABLED DISTRIBUTED RECEPTION

In this section, we will introduce the signal processing methods that can provide improved performance at the satellite-distributed receiver and enable AJ capability in the system.

A. Distributed-MRC for Optimal Receiver Combining

We consider the proposed receiver system, consisting of a ground terminal with T=1 antenna and S satellite nodes with one antenna each. All jammer-induced distortion is considered a strong external noise for implementing this scheme. In line with this assumption, looking back at the raw data symbols captured at each receiver in (1), for a satellite $i \in \{1, 2, \dots S\}$,

$$\mathbf{r}_i[k] = \sqrt{p_q} h_i \mathbf{x}[k] + \mathbf{n}_i. \tag{3}$$

The received data symbols from all the receivers can be written together as

$$\mathbf{R} = [\mathbf{r}_1^T[k], \mathbf{r}_2^T[k], \dots \mathbf{r}_S^T[k]]^T \in \mathbb{C}^{S \times \tau}.$$
 (4)

Since all S satellites are part of a distributed receiver, effective received data is obtained by combining the symbol frames captured at individual receivers. If $\mathbf{u} = [u_1, u_2, \dots u_S]^T$ is chosen as a weightage vector for this combining operation, $\mathbf{r}_{\text{combined}} \in \mathbb{C}^{1 \times \tau}$ is given as

$$\mathbf{r}_{\text{combined}} = \mathbf{u}^H \mathbf{R},$$
 (5)

where $(.)^H$ is a Hermitian operation.

d-MRC is a technique that provides optimal values for **u** with an aim to maximize the effective SNR:

$$SNR = \frac{p_g \sum_{i=1}^{S} ||u_i^H h_i||^2}{\sigma^2 \sum_{i=1}^{S} ||u_i^H||^2}.$$
 (6)

For maximizing SNR in (6), weights can be derived using the Cauchy-Schwarz inequality [15] as

$$\mathbf{u}_{\mathrm{d-MRC}} = \mathbf{h},\tag{7}$$

where σ^2 is the additive white Gaussian noise power level.

Therefore, using the weight vector **u** for combining data in the proposed system will optimize receiver data rates at the LEO nodes.

B. AJ Resilience using Distributed-LMMSE

Now, we look at the proposed system architecture, with an extra emphasis on the jammer-induced distortion. The sampled baseband data is represented using (1) to show the jammer's effect as an external interference explicitly. Thus, rewriting (1) and (4), for satellite $i \in \{1, 2, ... S\}$:

$$\mathbf{r}_i[k] = \sqrt{p_g} h_i \mathbf{x}[k] + \sqrt{p_j} h_{j,i} \mathbf{x}_j[k] + \mathbf{n}_i$$
 and $\mathbf{r}_{\text{combined}} = \mathbf{u}^H \mathbf{R}$.

The total effective signal-to-interference-plus-noise (SINR) is now given as:

SINR =
$$\frac{p_g \sum_{i=1}^{S} ||u_i^H h_i||^2}{\sigma^2 \sum_{i=1}^{S} ||u_i^H||^2 + p_j \sum_{i=1}^{S} ||u_i^H h_{j,i}||^2}.$$
 (8)

d-LMMSE method chooses an optimal value for u, which maximizes the SINR in (8). By solving this as a minimum mean square error optimization problem, we identify u that mitigates the effect of external jamming interference. So, SINR maximization can be re-written as:

$$\max_{\mathbf{u}} \text{SINR} = \min_{\mathbf{u}} E[||\mathbf{u}^{H}\mathbf{R} - \mathbf{x}||^{2}]. \tag{9}$$

where E[.] is the expectation operation. By assuming that the transmitted legitimate signals, jammer signals and additive noise are all mutually independent, i.e. $E[\mathbf{x}\mathbf{x}_j] = E[\mathbf{x}\mathbf{n}] = E[\mathbf{x}_j] = E[\mathbf{x}\mathbf{n}] = E[\mathbf{x}_j] = E[\mathbf{x}\mathbf{n}] = E[\mathbf{x}\mathbf{n}] = 0$, and simplifying the minimization problem using vector calculus, the optimal combining vector is obtained as shown below:

$$\mathbf{u}_{\text{d-LMMSE}} = p_q(p_q \mathbf{h} \mathbf{h}^H + p_i \mathbf{h}_i \mathbf{h}_i^H + \sigma^2)^{-1} \mathbf{h}.$$
 (10)

This combining method assumes that the jammer channel information \mathbf{h}_j is known during the weighting operation. In such a scenario, the d-MRC weight vector (\mathbf{u}_{d-MRC}) can be updated to incorporate the effect of jammer through the term $p_j\mathbf{h}_j\mathbf{h}_j^H$ in (10). However, in actual implementations, this value is not readily available, and thus, the effect of the jammer has to be estimated before applying the d-LMMSE combining method.

IV. USRP-BASED LEO EMULATION TESTBED

We developed a local testbed in an indoor laboratory using the USRP X310 SDRs to evaluate different signal-processing approaches. To stay true to the real-life implementations, the testbed was deployed in a lab without special equipment such as an anechoic chamber or RF absorbers.

Fig. 2 shows the actual hardware setup in our lab. One USRP X310, equipped with 2 UBX-40 daughterboards, was utilized to emulate the ground terminal transmitter (TX). This transmitter supports 2 outgoing data streams, but only one TX antenna was employed for evaluation purposes. Two X310s (RXs), equipped with 1 UBX-40 daughterboard each, were deployed to emulate the distributed LEO swarm receiver. Both TX and RXs were equipped with the VERT2450 isotropic antennas.

In any communication system, radio frontend systems on individual devices operate using uncorrelated local oscillators

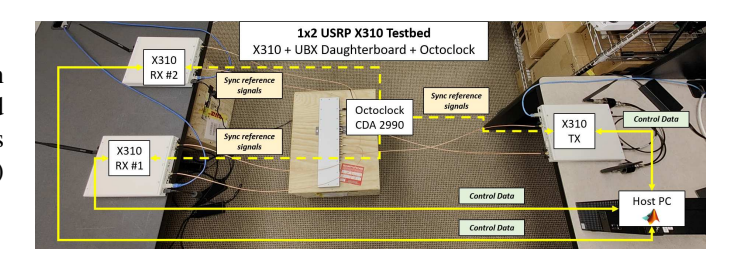


Fig. 2. Our USRP X310-based OTA testbed.

TABLE I COMMUNICATION PARAMETER SETUPS.

Value			
2.55 GHz			
1 MHz			
Uncoded QPSK			
2			
0.5			
-48 to -24 dBm			
101 samples of Zadoff-Chu Sequences			
1800 Symbols			

and clock sources. This results in frequency and timing offsets, which must be eliminated at the receivers for meaningful data processing. To ease such device synchronization issues, we employed a CDA-2990 Octoclock to provide a 10 MHz reference signal and 1 PPS pulse to the local oscillators of UBX-40 daughterboards. All the SDRs are connected to a host PC and are controlled using different MATLAB instances. We used the R2022b version of the software for our experiments. While the Octoclock provided frequency and timing reference signals to aid with synchronization, owing to the wireless propagation and oversampled transmission (2 samples/symbol), we performed a timing offset correction at individual receivers to extract the best sample when downsampling to symbol rate. All signal post-processing functions, such as matched filtering, timing offset correction, channel estimation, and payload extraction, were performed on individual MATLAB instances for the receiver SDRs.

We utilized a Rohde & Schwarz signal generator to implement a jammer, which transmitted different jamming signals out of a single VERT2450 antenna. In our evaluations, jammers are assumed to be on the ground when jamming the satellites in space. Therefore, a single jammer may potentially block the communication for a subset of all LEO nodes in a swarm. To depict this in the lab, we placed the jamming antenna very close to one of the receivers, such that any jamming signal only affects that node while having minimum impact on the second receiver.

TABLE I shows the communication parameters used in our evaluations. It has to be noted that we performed our experiments with transmit powers varying from noise floor to about 15 dB above it. Since various applications heavily occupy the ISM 2.4-2.5 GHz band, maintaining a constant noise floor for our experiments was difficult. So, we used the education broadband service spectrum band 2.55 GHz at

a small bandwidth to ensure negligible impact on licensed transmissions, if any. Also, all of our experiments use a block mode of communication, where data frames of size 1800 samples, preceded by a preamble sequence, are sent out from the ground terminal, and distributed LEO nodes capture the raw data independently for further processing.

A. Wireless Channel Characterization

One of the significant aspects of evaluating using an SDR testbed is to ensure that wireless channels emulate the satellite communication scenario. Since the testbed is not placed in any special anechoic chamber, all the testing is bound to be affected by severe multipath components due to reflections and diffractions from the surroundings. Therefore, the TX and RXs must have a strong LOS component in their physical setup and the wireless channel behavior. Another cornerstone to emulate is the diversity among different receiver channels.

To validate these attributes, we started by first estimating the channel as a single-tap filter. Then, we performed the following two analyses: using a Rician channel model to extract the K-factor from IQ samples and verify the diversity by showing uncorrelated channels at both receivers.

1) Single-tap Filter Channel: We employed a preambleenabled data transmission as seen from TABLE I. We exploited the excellent autocorrelation properties of Zadoff-Chu sequences to get a one-tap estimate of the channel response. If x[k] represents the transmitted preamble sequence and r[k]represents the captured preamble symbols, then a channel estimate is obtained as [17]:

$$\hat{h} = \max\left(\operatorname{corr}(r[k], x[k])\right). \tag{11}$$

2) Rician K-factor Extraction: A Rician channel is a statistical model characterized to have an LOS component and a fading component. The value of its K-factor determines the dominance of this component over the fading counterparts. A higher K-factor represents a more substantial LOS component. We estimated the K-factor from different IQ samples captured at the receivers and compared them against different transmit powers in the range shown in TABLE I. A second-order moment-based estimation of Rician K-factor was utilized in our experiments [19], [20]:

$$K = \frac{\sqrt{1 - \gamma}}{1 - \sqrt{1 - \gamma}},$$

$$\gamma = V[\mathbf{r}^2]/E[\mathbf{r}^2]^2$$
(12)

$$\gamma = V[\mathbf{r}^2]/E[\mathbf{r}^2]^2 \tag{13}$$

where V[.] here represents the variance of received power, and E[.] represents the received power, both calculated from the captured symbols $\mathbf{r}[k]$.

It should be noted that, concerning a particular ground terminal, a satellite has robust LOS only for a specific duration of its orbit. As it moves closer to the horizon, the LOS probability reduces (with varying magnitudes in urban and rural areas) [9]. To demonstrate this in an indoor lab, we chose a range of transmission power levels to move from LOSdominant communication to multipath component-dominant

TABLE II RICIAN K-FACTOR FOR TWO RECEIVERS: RX1 AND RX2.

TX Power (dBm)	K-factor		
	RX1	RX2	
-48	5.50	6.07	
-42	8.20	8.76	
-36	17.51	20.04	
-30	39.70	44.53	
-24	71.81	74.72	

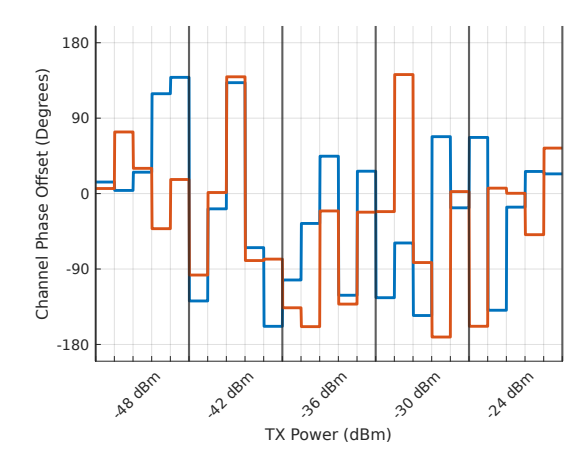


Fig. 3. Variation of channel phase offsets for different iterations of data capture.

communication. TABLE II shows the variation of K-factor for different operating regions.

3) Channel Phase Offset Comparison: LEO satellites acting as distributed receiver nodes will aid data rate enhancement and AJ resilience only when their channels are uncorrelated. Therefore, when implementing a testbed, it is imperative to verify this behavior before performing further signal processing. Owing to their nature, single-tap channels induce a constant phase offset during data propagation. However, this offset should differ for all receiver channels if channels are uncorrelated. Therefore, to prove that the two receiver channels are uncorrelated, we show that the phase offsets induced by the estimates are significantly different. These results agree with the theoretical understanding of channels being uncorrelated if the receiving antennas are apart by more than half the carrier wavelength $(c_0/2f_c \approx 6 \, \text{cm})$ as well (fig. 2 shows that receivers are much further apart in the testbed).

Fig. 3 shows the variation of phase offsets induced due to the two receiver channels at different operating points. It is evident here that the channel phase offsets are very different for both the receivers at most operating points. Since the receiver nodes are relatively equidistant from the ground terminal, similarity in channel magnitudes is plausible. However, the receiver channels will remain uncorrelated due to different phase offsets, which will be shown later to aid in diversity-enabled optimal combining schemes.

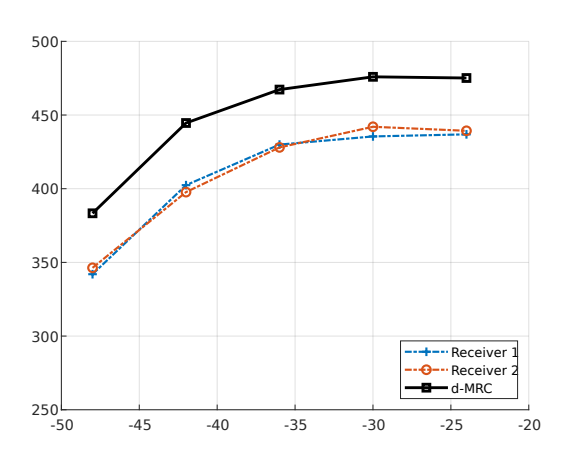


Fig. 4. Performance improvement in data rate via d-MRC.

V. OVER-THE-AIR PERFORMANCE EVALUATION

After proving that our testbed setup can emulate satellite channels in an indoor environment, we show the effectiveness of our combining schemes that provide diversity-enabled data rate enhancement and AJ resilience on our testbed. d-MRC provides an improved performance in terms of data rates over SISO operation. d-LMMSE improves upon d-MRC and SISO in the presence of an external jammer. For evaluating these algorithms, we conducted block-data transfers based on the parameters shown in TABLE I. Also, it is essential to note that we utilized a GNU Radio-powered spectrum analyzer [21] on both receivers in the testbed to measure the received signal power relative to the noise floor and positioned the SDRs such that both receiver nodes get similar power levels when transmitting data. These measurements show that for a noise floor of -128 dB, varying the transmit power in [-48 dBm, -24 dBm] corresponded to a received signal power in the range of [-108 dB, -127 dB].

Fig. 4 shows the physical-layer data rates of individual receivers (in Kbps) and how the d-MRC scheme improves upon the SISO data rates by exploiting the channel estimates and performing a receiver diversity-based combining. d-MRC shows a distinct improvement in the combined data rate against either of the receivers across all operating points.

Now, before conducting OTA experiments to incorporate jamming and evaluate the d-LMMSE scheme, upon referring to (10), it is necessary to compute an approximation for the jammer and noise-dependent term in the weight vector $(p_j\mathbf{h_j}\mathbf{h_j}^H+\sigma^2)$. On close observation, this term represents the summation of the jammer signal power level and noise power, as captured at the receivers. We calculated an approximation to this term by performing a time division multiplexing-based data capture. Here, the receivers would first capture a set of raw IQ samples without legitimate transmission before capturing them again during legitimate OTA experiments. Using this principle, the raw samples would consist of only jammergenerated IQ samples and noise in the first data capture. At

TABLE III
RICIAN K-FACTOR FOR THE RECEIVERS AFTER JAMMING.

TX Power (dBm)	Noise floor			
	-125 dB		-120	dB
	RX1	RX2	RX1	RX2
-48	4.64	6.05	3.60	6.04
-42	6.30	8.06	4.44	7.91
-36	10.27	17.92	7.09	16.38
-30	24.61	41.01	13.11	34.44
-24	46.44	63.20	35.05	52.33

satellite i such that $i \in [1, 2]$:

$$\hat{\mathbf{r}}_i[k] = \sqrt{p_i} h_{i,i} \mathbf{x}_i[k] + \mathbf{n}_i, \tag{14}$$

and data captured at both receivers together in our testbed is given as

$$\hat{\mathbf{R}} = [\hat{\mathbf{r}}_1^T[k] \quad \hat{\mathbf{r}}_2^T[k]]^T$$

$$= \sqrt{p_i} \mathbf{h}_i \mathbf{x}_i + \mathbf{N}$$
(15)

where $\mathbf{h}_j = [\mathbf{h}_{j,1}, \mathbf{h}_{j,2}]^T$, and $\mathbf{N} = [\mathbf{n}_1^T, \mathbf{n}_2^T]^T$. If the IQ samples generated at the jammer $(\mathbf{x}_j[k])$ are assumed to have unit power, then a crude approximation for the jammer-plusnoise-power term earlier is given as $\hat{\mathbf{R}}\hat{\mathbf{R}}^H$:

$$\hat{\mathbf{R}}\hat{\mathbf{R}}^H = \tau \, p_q h_j h_i^H + \mathbf{N}\mathbf{N}^H + A. \tag{16}$$

 $A = \sqrt{p_j} (\mathbf{h}_j \mathbf{x}_j \mathbf{N}^H + \mathbf{N} \mathbf{x}_j^H \mathbf{h}_j^H)$ is an extra component, which will have a small implication if the jammer is very strong compared to the additive noise.

With this approximation in hand, we introduce an external interference into the environment by employing the signal generator. A OPSK jammer, which transmits random symbols modulated as QPSK data, was set to operate with constant power across the entire communication bandwidth of 1 MHz. To emulate the practical use case where a subset of the LEO swarm may jammed by a ground-located jammer, only one of the receiver nodes (RX1) was jammed very firmly using the signal generator while having a minimum effect on the second receiver (RX2). We conducted the OTA experiments for two jammer power levels, which will raise the noise floor of RX1 from -128 dB to -125 dB and -120 dB, respectively. TABLE III shows the effect of jamming on LOS dominance due to the raised noise floor. It can be seen that RX1 has much lower K-factor values, indicating that it suffered higher attenuation than RX2 from the jammer.

Fig. 5 and Fig. 6 show the performance of d-MRC and d-LMMSE combining schemes in the presence of a strong jammer at RX1. It can be observed that RX1 data rates have plummeted compared to the experiment without any external jammer (Fig. 4). And, as the jammer power increases, the difference in SISO performance for both receivers increases. Looking at d-MRC curves, since it relies on LOS channel estimates alone for its weighting operation, its performance deteriorates slightly at high jammer power. In contrast, d-LMMSE can utilize the jammer channel information to improve the weight vector updates as shown in (10). This is also clearly evident from the d-LMMSE curves in the figures,

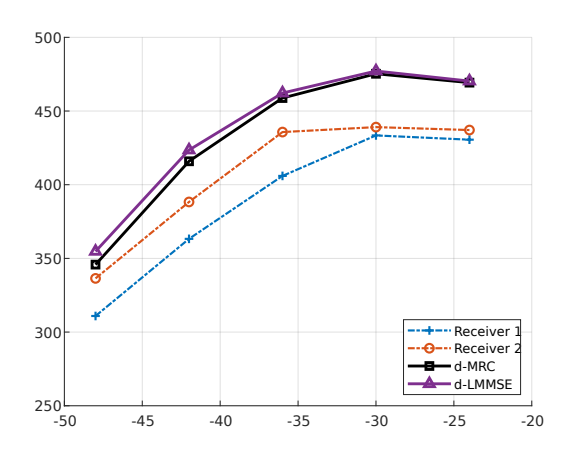


Fig. 5. Data rates when QPSK jammer pushes noise floor to -125 dB.

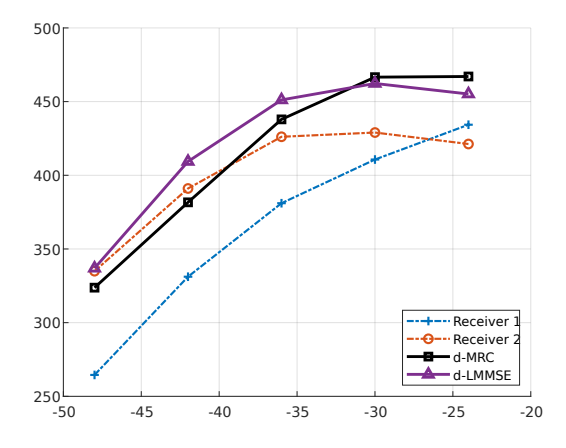


Fig. 6. Data rates when QPSK jammer pushes noise floor to -120 dB.

where it has overperformed both SISO and d-MRC at almost all operating points. Also, this scheme is effective, particularly at low transmit powers, which corresponds to low SINR ratios. Therefore, d-LMMSE can build robustness into a LEO satellite swarm system, especially at low SINRs.

VI. CONCLUSION

In this paper, we proposed a LEO satellite swarm architecture that can implement a distributed receiver system to mitigate the lack of diversity in satellite channels. We then introduced two algorithms for improving the overall data rate and building anti-jamming capability on this framework. First, d-MRC performs an optimal combining operation for distributed nodes by exploiting the LOS channel estimates. Second, d-LMMSE builds AJ resilience by leveraging the jammer channel information and legitimate channel estimates. Finally, we developed a hardware testbed using the USRP X310s and demonstrated the possibility of emulating satellite channels indoors; we also proved the effectiveness of d-MRC and d-LMMSE schemes on actual OTA data.

REFERENCES

- S.-C. Lin, C.-H. Lin, L. C. Chu, and S.-Y. Lien, "Enabling resilient access equality for 6g leo satellite swarm networks," *IEEE Internet of Things Magazine*, vol. 6, no. 3, pp. 38–43, 2023.
- [2] "Technical specification group radio access network; solutions for nr to support non-terrestrial networks (ntn) (release 16)," 3rd Generation Partnership Project, Tech. Rep. 3GPP TR 38.821 V16.1.0, 2021.
- [3] Z. Qu, G. Zhang, H. Cao, and J. Xie, "Leo satellite constellation for internet of things," *IEEE Access*, vol. 5, pp. 18391–18401, 2017.
- [4] C. Li, Y. Zhang, R. Xie, X. Hao, and T. Huang, "Integrating edge computing into low earth orbit satellite networks: architecture and prototype," *IEEE Access*, vol. 9, pp. 39126–39137, 2021.
- [5] "Space development agency one pager," 2023. [Online]. Available: https://www.sda.mil/wp-content/uploads/2023/05/SDA_One-Pager_Update_FINAL.pdf
- [6] H. Al-Hraishawi, H. Chougrani, S. Kisseleff, E. Lagunas, and S. Chatzinotas, "A survey on non-geostationary satellite systems: the communication perspective," *IEEE Communications Surveys & Tutori*als, pp. 1–1, 2022.
- [7] M. Röper, B. Matthiesen, D. Wübben, P. Popovski, and A. Dekorsy, "Beamspace mimo for satellite swarms," in 2022 IEEE Wireless Communications and Networking Conference (WCNC), 2022, pp. 1307–1312.
- [8] O. Kodheli, E. Lagunas, N. Maturo, S. K. Sharma, B. Shankar, J. F. M. Montoya, J. C. M. Duncan, D. Spano, S. Chatzinotas, S. Kisseleff, J. Querol, L. Lei, T. X. Vu, and G. Goussetis, "Satellite communications in the new space era: a survey and future challenges," *IEEE Communications Surveys & Tutorials*, vol. 23, no. 1, pp. 70–109, 2021.
- [9] "Technical specification group radio access network; study on new radio (nr) to support non-terrestrial networks (release 15)," 3rd Generation Partnership Project, Tech. Rep. 3GPP TR 38.811 V15.4.0, 2020.
- [10] P. Yue, J. An, J. Zhang, J. Ye, G. Pan, S. Wang, P. Xiao, and L. Hanzo, "Low earth orbit satellite security and seliability: issues, solutions, and the road ahead," *IEEE Communications Surveys & Tutorials*, vol. 25, no. 3, pp. 1604–1652, 2023.
- [11] V. Weerackody, "Satellite diversity to mitigate jamming in leo satellite mega-constellations," in 2021 IEEE International Conference on Communications Workshops (ICC Workshops), 2021, pp. 1–6.
- [12] S. P. Winter, C. A. Hofmann, and A. Knopp, "Antenna diversity techniques for enhanced jamming resistance in multi-beam satellites," in *MILCOM* 2016 - 2016 IEEE Military Communications Conference, 2016, pp. 618–623.
- [13] M. F. Pervej and S.-C. Lin, "Eco-vehicular edge networks for connected transportation: A distributed multi-agent reinforcement learning approach," in 2020 IEEE 92nd Vehicular Technology Conference (VTC2020-Fall), 2020, pp. 1–7.
- [14] S.-C. Lin, L. Gu, and K.-C. Chen, "Providing statistical qos guarantees in large cognitive machine-to-machine networks," in 2012 IEEE Globecom Workshops. IEEE, 2012, pp. 1700–1705.
- [15] R. W Heath Jr., Introduction to wireless digital communication: a signal processing perspective, 1st ed. Pearson Education, 2017.
- [16] J. Ma, C. Peng, S.-C. Lin, and T. Qiu, "Asynchronous blind modulation classification in the presence of non-gaussian noise," in 2019 IEEE International Symposium on Dynamic Spectrum Access Networks (DySPAN), 2019, pp. 1–10.
- [17] V. S. R. Kantheti, S.-C. Lin, and L. C. Chu, "Spels: Scalable and programmable testbed for evaluating leo satellite swarm communications," in *IEEE INFOCOM 2023 - IEEE Conference on Computer Communications Workshops (INFOCOM WKSHPS)*, 2023, pp. 1–6.
- [18] L. J. Ippolito Jr., Satellite communications system engineering: atmospheric effects, satellite link design and system performance. John Wiley and Sons, Ltd, 2008.
- [19] A. Abdi, C. Tepedelenlioglu, M. Kaveh, and G. Giannakis, "On the estimation of the k parameter for the rice fading distribution," *IEEE Communications Letters*, vol. 5, no. 3, pp. 92–94, 2001.
- [20] J.-J. Park, M.-D. Kim, H.-K. Chung, and W. Kim, "Ricean k-factor analysis of indoor channel measurements at 3.7 ghz," in 2010 5th International ICST Conference on Communications and Networking in China, 2010, pp. 1–5.
- [21] "Creating a software radio spectrum analyzer," 2023. [Online]. Available: https://wiki.gnuradio.org/index.php/Guided_Tutorial_Hardware_Considerations